Young's modulus identification via finite element model updating using full-field data from a 3-point bending test

Arthur M. Gonçalves[1], Igor P. Zago[2], Rafael Vargas[3], Rodrigo B. Canto[2,4], Ricardo A. Angélico[1]

[1]*Department of Aeronautical Engineering, São Carlos School of Engineering, University of São Paulo*
Av. João Dagnone, 1100, Santa Angelina, 13563-120, São Carlos/SP, Brazil
arthurg@usp.br, raa@sc.usp.br
[2]*Graduate Program in Materials Science and Engineering – PPGCEM, Federal University of São Carlos*
Rod. Washington Luis, km 235, 13565-905, São Carlos/SP, Brazil
ipzago@estudante.ufscar.br
[3]*Univ Lyon, INSA Lyon, Université Claude Bernard Lyon 1, CNRS*
MATEIS, UMR5510, 69621 Villeurbanne, France
rafael.vargas-maginador@insa-lyon.fr
[4]*Dept. of Materials Engineering, Federal University of São Carlos*
Rod. Washington Luis, km 235, 13565-905, São Carlos/SP, Brazil
rbcanto@ufscar.br

Abstract. High-temperature applications demand materials with adequate properties to withstand this harsh condition, where the optimal choice for such applications is often refractory materials. The mechanical design of structures with such materials demands their properties to be well characterized. Non-intrusive image-based techniques are welcome to investigate these material properties, allowing full-field displacement measurements. In this context, this article aims to assess Young's modulus of refractory material by combining Digital Image Correlation (DIC) and a Finite Element Model Updating (FEMU) approach. DIC allows the identification of the displacement field over a region of interest for each loading level (i.e., acquired image). Images were gathered through a camera setup in a 3-point bending test, and the DIC analysis was performed in MATLAB® with the Correli framework. The identification problem was modeled using finite element software Abaqus and its Scripting Interface in Python. A sensitivity analysis was performed to ensure the successful identification of parameters. Then, the elastic parameters were iteratively updated until computational results matched the experimental displacement field (FEMU-U), within a tolerance. The displacement residue involving the comparison of the computational model and experimental results was discussed. It is shown that the richness of full-field measurements is helpful in identifying parameters from a single experiment.

Keywords: Digital Image Correlation; Finite Element Model Updating; Parameter identification.

1 Introduction

As stated by Lee et al. [1], refractory ceramics are widely used as thermal insulators in high-temperature industrial applications. Vargas et al. [2] highlighted the importance of investigating the elastic properties and fracture behavior of refractories to optimize their lifespan and safety in service. Hild and Roux [3] concluded that there are limited possibilities of mechanical testing for this purpose. In fact, according to Gogotsi [4], ceramics tend to suffer a considerable decay in their tensile strength at high-temperatures, and their fracture can be highly destructive. As a result, testing these materials in such conditions requires non-invasive measurement techniques that preserve the integrity of the specimen and the instrumentation, while being capable of detecting small displacements.

Over the past few decades, numerous techniques have been developed for the experimental identification of the elastic properties of several types of materials. Some of them were investigated by Pengjin et al. [5], their particularities for use in brittle materials being summarized. For example, Cui et al. [6] demonstrated the difficulty of acquiring data using traditional methods and sensors, such as strain gauges and extensometers, in tests at high-temperatures for long periods. Furthermore, such methods have the disadvantage of producing results based on the local mechanical response of the material, which may not account for the difficulties (or impossibilities) of knowing where damage will start.

Therefore, it is desirable that the mechanical testing of ceramic materials at high-temperatures is carried out using non-contact measurement methods capable of analyzing the entire surface of the specimen. In this context, Schreier et al. [7], Hild and Roux [8] showed that the Digital Image Correlation (DIC) technique is an excellent option. This method consists of analyzing images of a specimen surface in different loading states. The displacements at various points of the texture can then be digitally evaluated over time to obtain experimental field information, as stated by Pierron et al. [9].

Avril et al. [10], and Ruybalid et al. [11] demonstrated how parameters of interest can be identified by iteratively updating a finite element (FE) model and comparing its outputs to experimental data obtained using DIC. The parameters are successfully identified when the minimization between the numerical model and experimental results converges. The authors go further in calling this method FEMU-U when the displacement field is the minimized output. The present article applies FEMU-U to identify Young's modulus of a ceramic specimen with full-field measurements.

2 Experimental test assisted by DIC

In this paper, a 3-point bending test was used to evaluate the elastic properties of a ceramic specimen. This test is often used to evaluate elastic and fracture parameters of brittle materials as observed in the works of Fang et al. [12] and Vargas et al. [13]. The test setup is shown in Fig. 1, which is similar to that described in the ASTM Standard C293, 2016 [14]. A region of interest (ROI), where DIC is performed, is established to eliminate the interference of borders. The tested specimen was an alumina bar with dimensions 150x25x25 mm^3. Images were acquired during the experiment, and the load data was recorded by the testing machine.

The first step in carrying out the test was to apply a random speckle in the specimen's surface, whose importance is to help with convergence, as highlighted by Vargas et al. [15]. The texture consists of a ceramic slip that withstands temperatures up to $900°C$ and contrasts with the specimen, contributing to a wider dynamic range for the images.

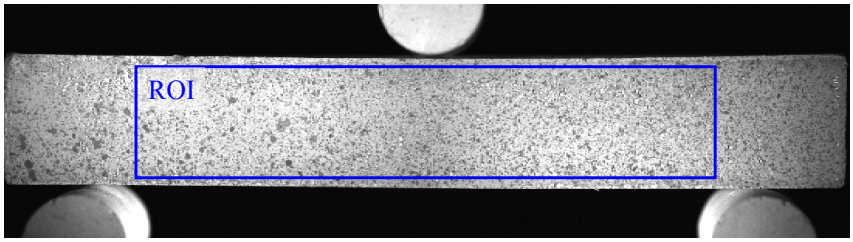

Figure 1. Image of the 3-point bending test, where the ROI is delimited by the blue line.

The experiment was conducted according to the flowchart in Fig. 2 and controlled by the universal testing machine MTS (Exceed E44.304 model), with TestSuite™ software. Initially, a preload of 40 N was applied to ensure the specimen positioning. Then, ten reference images were acquired for uncertainty analysis, with a 10-second interval between each one. After that, a progressive loading was applied at a rate of 0.01 mm min^{-1} until 79 images were captured using a Canon EOS 5DS camera, with 1 pixel corresponding to 37.2 μm in the images.

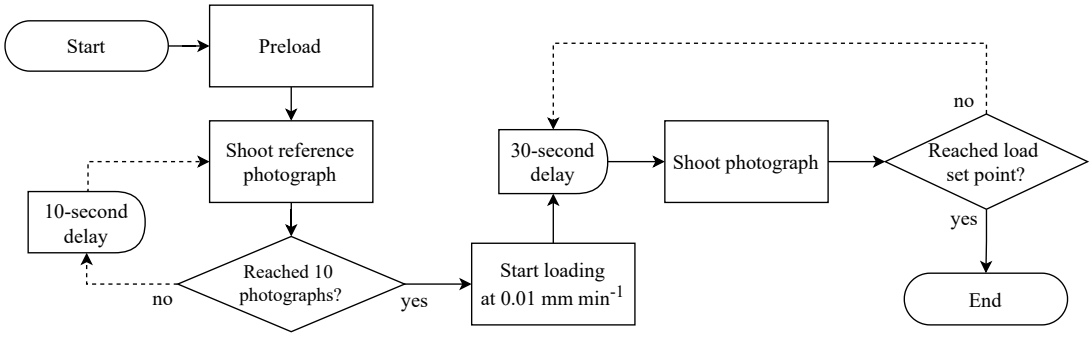

Figure 2. Flowchart describing the testing procedure and image acquisition. The preload was set to 40 N, and the maximum reached load was 205 N, after which the specimen cracked.

3 Computational methods

Figure 3 shows the 2D Abaqus FE model representative of the experiment (i.e., with matching dimensions and boundary conditions). The concentrated force at the top of the specimen is the same as the test's ultimate load, which was measured as 205 N. Note that, to ensure compatibility, the same ROI mesh was used for both the model and the DIC analysis.

In this study, the translations of the experiment were removed from the DIC results before the data post-processing. This was made to allow a compatibility between the DIC and FE results. The procedure employed was to select a node in the mesh center as a reference for the translations by subtracting this node displacement from all nodes in the system. Therefore, the results presented here will show the relative displacement fields to the reference node. Additionally, both of the 3-point bending test lower supports were leveled during the experiment. Hence, two vertical displacement restraints were modeled near the edges at the bottom side of the specimen to reproduce the referred supports. A horizontal restraint was placed to remove the remaining rigid-body DOF.

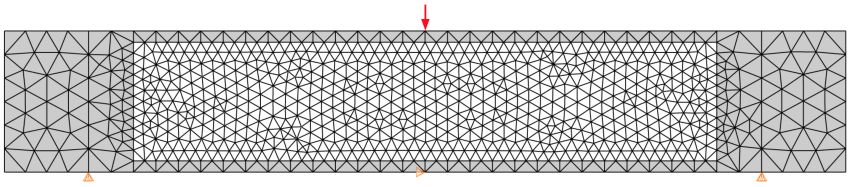

Figure 3. Abaqus FE model. The brighter, denser region at the center corresponds to the DIC ROI.

3.1 Digital Image Correlation (DIC)

The experimental displacement field was determined with DIC, by comparing images of the ROI obtained in different states of deformation. The comparison is made between a reference image, $f(\mathbf{x})$, and a deformed image, $g(\mathbf{x})$. They can be interpreted as a distribution of gray levels as a function of spatial coordinates $\mathbf{x}$.

The images are correlated after a correction made by a field of displacements $\mathbf{u}(\mathbf{x})$:

$$f(\mathbf{x}) = g(\mathbf{x} + \mathbf{u}(\mathbf{x})). \tag{1}$$

Considering that the reference image is differentiable, eq. (1) may be approximated by a first-order Taylor series expansion,

$$\tilde{g}(\mathbf{x}) = g(\mathbf{x}) + \mathbf{u}(\mathbf{x}) \cdot \boldsymbol{\nabla} g(\mathbf{x}), \tag{2}$$

and the estimation of $\mathbf{u}$ consists of minimizing the quadratic difference between $f(\mathbf{x})$ and $\tilde{g}(\mathbf{x})$ over the region of interest, herein designated as Ω, which results in

$$\gamma^2 = \iint_{\Omega} [f(\mathbf{x}) - g(\mathbf{x}) - \mathbf{u}(\mathbf{x}).\boldsymbol{\nabla} g(\mathbf{x})]^2 \, d\Omega, \tag{3}$$

where γ^2 is the correlation's residue.

The software used in the article, Correli 3.2, with previous versions licensed under [16], interpolates the distribution of gray levels, providing a means of determining displacements with sub-pixel resolution. To do so, it employs an FE-based method, using linear T3 finite element shape functions, $\boldsymbol{\Psi}$, to approximate the displacement field, which becomes

$$\mathbf{u}(\mathbf{x}) = \sum_i u_i \boldsymbol{\Psi}_i(\mathbf{x}), \tag{4}$$

where i indicates the degrees of freedom (DOF) associated with the ROI. Naturally, the double integral in eq. (3) is also approximated by a discrete summation over Ω.

The Correli 3.2 framework provides a series of functions allowing users to customize the correlation procedure according to their needs. The software was developed and continues to be worked on by the Eikologie

team led by François Hild and Stéphane Roux from the "Laboratoire de Mécanique Paris-Saclay" (LMPS). More information about it and its applicability for field measurements is available in papers published by Hild, Roux and their research group [3, 17].

3.2 Finite Element Model Updating (FEMU)

Identifying a set of parameters of interest, $\{\mathbf{p}\}$, can be performed by minimizing the difference between the Abaqus FE model and the results obtained experimentally through DIC. To this end, as explored by Vargas [18], the cost function can take one form in particular, FEMU-U, which was used throughout this project. The algorithm was built in Python using the Abaqus Scripting Interface and iteratively updated through a MATLAB® script.

FEMU-U procedure considers the minimization of the quadratic difference between $\{\mathbf{u}_{exp}\}$ and $\{\mathbf{u}_{FE}\}$, the vectors gathering all experimental and computational degrees of freedom, respectively. Being n_{DOF} the number of DIC-related degrees of freedom (DOF), then

$$\chi^2_U(\{\mathbf{p}\}) = \frac{1}{\gamma_U^2 \cdot n_{DOF}} \sum_{i=1}^{n_{DOF}} \Big[u_{i,exp} - u_{i,FE}(\{\mathbf{p}\})\Big]^2, \tag{5}$$

where γ_U is the uncertainty associated with the displacement field. As acknowledged by Mathieu et al. [19], normalization by γ_U suggests that when the difference between $\{\mathbf{u}_{exp}\}$ and $\{\mathbf{u}_{FE}\}$ is only due to the noise acquisition inherent to the experiment, χ_U tends to unity.

Once the experimental data was post-processed by DIC and the finite element model was created, the first step in implementing FEMU was to calculate and study the sensitivity matrix

$$[\mathbf{S_U}] = \frac{1}{\gamma_U}\left[\frac{\partial \mathbf{u}_{FE}}{\partial p_i}(\{\mathbf{p}\})\right], \tag{6}$$

which describes how sensitive $\{\mathbf{u}_{FE}\}$ is to each calibration parameter, p_i. The derivative with respect to the parameter p_i is herein approximated using a first-order finite difference with a perturbation of 1% of p_i.

Next, the minimization of eq. (5) is performed iteratively updating the parameters by solving the system

$$[\mathbf{H_U}]\{\delta\mathbf{p}\} = \{\mathbf{h_U}\}, \tag{7}$$

where $[\mathbf{H_U}]$ is the Hessian matrix,

$$[\mathbf{H_U}] = [\mathbf{S_U}]^T[\mathbf{S_U}], \tag{8}$$

$\{\mathbf{h_U}\}$ is given by

$$\{\mathbf{h_U}\} = [\mathbf{S_U}]^T\left\{\frac{\mathbf{u}_{exp} - \mathbf{u}_{FE}(\{\mathbf{p}^{(\mathbf{n})}\})}{\gamma_U}\right\}, \tag{9}$$

and $\{\delta\mathbf{p}\}$ updates the parameters of the current iteration, $\{\mathbf{p}^{(\mathbf{n})}\}$.

4 Results

The vertical component of the displacement field, $u_{y,exp}$, obtained with DIC for an applied loading of 205 N is displayed in Fig. 4. The displacement is shown in μm, and each pixel corresponds to 37.2 μm. Note that since the specimen is brittle and does not withstand high-stress levels, a low force was applied, leading to a maximum displacement of 21.4 μm vs. a standard deviation across the reference photos of 0.81 μm. Additionally, the residue distribution is uniform, ranging from -1 to 1% of the ROI's dynamic range, suggesting that the correlation was indeed successful. The global gray-level residue normalized by the ROI's dynamic range was 0.0052.

Horizontal and vertical displacement sensitivity fields to a variation of 1% of E can be seen in Fig. 5. As expected, both components are more sensitive near the tips, and the selected ROI is large enough to capture these changes. Initially, the identification procedure was idealized concerning the identification of the elastic modulus and Poisson's ratio. The Hessian matrix was computed for these parameters and normalized by the DIC's displacement noise. Only E showed to be identifiable because its corresponding value in the Hessian is way greater than the noise. All other fields depending on ν are too small and consequently ill-conditioned, as addressed by Roux and Hild [20]. Thus, the following results enclose only the identification of the elastic modulus.

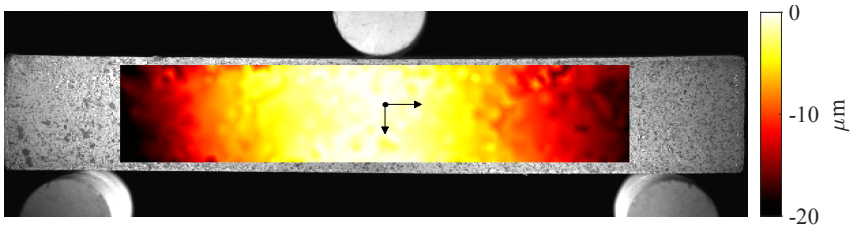

Figure 4. Vertical component u_{exp} for a load of 205 N. The displacements are measured with a coordinate system centered in the ROI.

(a) Horizontal displacement sensitivity field, normalized by γ_U. Scale in $1/\varepsilon$, where $\varepsilon = 0.01$ is the variation of E.

(b) Vertical displacement sensitivity field, normalized by γ_U. Scale in $1/\varepsilon$, where $\varepsilon = 0.01$ is the variation of E.

Figure 5. Sensitivity fields to a 1% variation of E.

FEMU-U was applied for all experimental loading levels (i.e., acquired images) independently, resulting in the identification distribution from Fig. 6 for an imposed Poisson ratio $\nu = 0.30$. It is important to highlight that several values of the Poisson ratio have been tested, and no significant changes were observed in the identified Young modulus. The average elastic modulus is set to 15.9 GPa with a standard deviation of 3.1 GPa. Finite element analysis using these properties resulted in the vertical displacement shown in Fig. 7a for an applied load of 205 N. The difference between the numerical model and the experimental test is displayed in Fig. 7b.

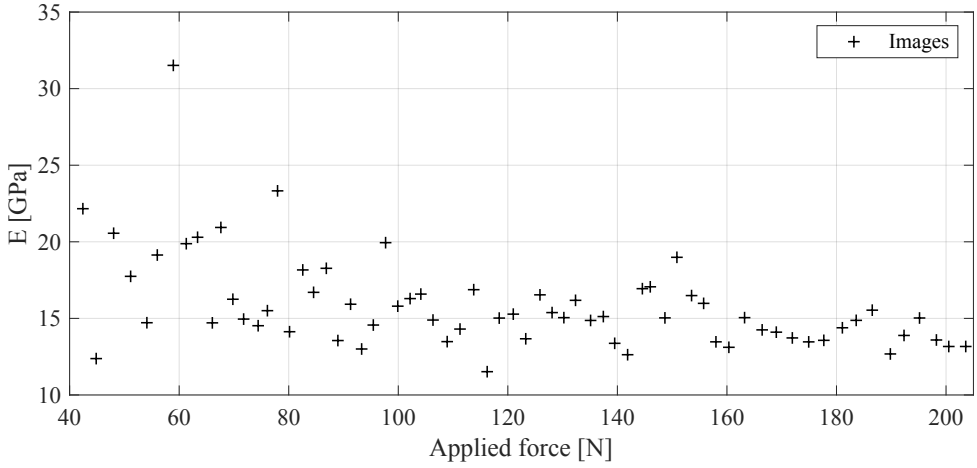

Figure 6. Identified elastic modulus for each captured image.

(a) Identified displacement field's vertical component.

(b) Difference between the vertical displacement of the experimental measurement and finite element model values.

Figure 7. Displacement from finite element model and the difference between the displacements fields of Abaqus model and experiment.

5 Conclusions

In this study, the Young's modulus of a ceramic specimen was satisfactorily identified as 15.9 GPa through a 3-point bending test assisted by the Digital Image Correlation (DIC) technique combined with a finite element model. A sensitivity analysis regarding the main elastic properties revealed that the Poisson's ratio could not be properly identified in this context. Alternative tests, such as the uniaxial compression test, may prove to be more effective. Further analysis introducing new parameters to the identification procedure concerning rotation and boundary conditions can be performed to investigate their influence on the identified Young modulus.

Acknowledgements. The authors would like to acknowledge the financial support of FAPESP through Processes #2023/13594-8 and #2020/08077-6, and also, CNPq processes 309266/2022-0 and 140250/2020-4, which allowed the current research and backed the development of tools needed for the experiments. This study was financed in part by the Coordenação de Aperfeiçoamento de Pessoal de Nível Superior - Brasil (CAPES) - Finance Code 001.

Authorship statement. The authors hereby confirm that they are the sole liable persons responsible for the authorship of this work, and that all material that has been herein included as part of the present paper is either the property (and authorship) of the authors, or has the permission of the owners to be included here.

References

[1] W. E. Lee, W. Vieira, S. Zhang, K. G. Ahari, H. Sarpoolaky, and C. Parr. Castable refractory concretes. *International Materials Reviews*, vol. 46, pp. 145–167, 2013.
[2] R. Vargas, J. Neggers, R. B. Canto, J. A. Rodrigues, and F. Hild. Analysis of wedge splitting test on refractory castable via integrated DIC. *Journal of the European Ceramic Society*, vol. 36, pp. 4309–4317, 2016.
[3] F. Hild and S. Roux. Measuring stress intensity factors with a camera: Integrated Digital Image Correlation (I-DIC). *Comptes Rendus Mécanique*, vol. 334, pp. 8–12, 2006a.
[4] G. A. Gogotsi. *Brittleness Measure of Ceramics*. Springer, Dordrecht, 2014.
[5] Y. Pengjin, M. Shengjun, M. Yuting, Y. Wenxuan, and S. Xiangfan. Multi-dimensional non-uniform deformation and failure of siltstone determined using acoustic, 3D-Digital Image Correlation, and computed tomography. *Theoretical and Applied Fracture Mechanics*, vol. 125, pp. 103800, 2023.
[6] Y. Cui, X. Li, T. Zhang, W. Ding, and J. Yin. Development of high-temperature wire-grid thin film strain gauges. *Sensors (Basel, Switzerland)*, vol. 22, 2022.
[7] H. Schreier, J. J. Orteu, and M. A. Sutton. *Image correlation for shape, motion and deformation measurements: Basic concepts, theory and applications*. Springer US, 2009.
[8] F. Hild and S. Roux. Digital Image Correlation: From displacement measurement to identification of elastic properties – A review. *Strain*, vol. 42, pp. 69–80, 2006b.

[9] F. Pierron, M. A. Sutton, and V. Tiwari. Ultra high speed DIC and virtual fields method analysis of a three point bending impact test on an aluminium bar. *Experimental Mechanics*, vol. 51, pp. 537–563, 2011.
[10] S. Avril, M. Bonnet, A. S. Bretelle, M. Grediac, F. Hild, P. Ienny, F. Latourte, D. Lemosse, S. Pagano, E. Pagnacco, and A.-S. Bretelle. Overview of identification methods of mechanical parameters based on full-field measurements. *Experimental Mechanics*, vol. 48, 2008.
[11] A. P. Ruybalid, J. P. Hoefnagels, van der O. Sluis, and M. G. Geers. Comparison of the identification performance of conventional FEM updating and integrated DIC. *International Journal for Numerical Methods in Engineering*, vol. 106, pp. 298–320, 2016.
[12] X. Fang, J. Jia, and X. Feng. Three-point bending test at extremely high temperature enhanced by real-time observation and measurement. *Measurement*, vol. 59, pp. 171–176, 2015.
[13] R. Vargas, I. P. Zago, V. F. Sciuti, M. Furlan, R. A. Angélico, F. Hild, and R. B. Canto. Multi-window setup for thermomechanical experiments assisted by DIC up to 900°C. *Materials Research*, vol. 27, 2024.
[14] ASTM Standard C293, 2016. *Standard test method for flexural strength of concrete (using simple beam with center-point loading)*. ASTM International, West Conshohocken, PA, 2016.
[15] R. Vargas, R. Canto, F. Hild, and S. Roux. On accounting for speckle extinction via DIC and PCA. *Optics and Lasers in Engineering*, vol. 149, pp. 106813, 2022.
[16] H. Leclerc, J. Neggers, F. Mathieu, F. Hild, and S. Roux. Correli 3.0 [IDDN.FR.001.520008.000.S.P.2015.000.31500]. Agence pour la Protection des Programmes, Paris (France), 2015.
[17] J. Neggers, F. Mathieu, F. Hild, S. Roux, and N. Swiergiel. Improving full-field identification using progressive model enrichments. *International Journal of Solids and Structures*, vol. 118-119, pp. 213 – 223, 2017.
[18] R. Vargas. *Fracture of refractories at room and elevated temperatures analyzed with wedge splitting tests and image correlation*. PhD thesis, Federal University of São Carlos, São Carlos, 2024.
[19] F. Mathieu, H. Leclerc, F. Hild, and S. Roux. Estimation of elastoplastic parameters via weighted FEMU and Integrated-DIC. *Experimental Mechanics*, vol. 55, pp. 105–119, 2015.
[20] S. Roux and F. Hild. Comprehensive full-field measurements via Digital Image Correlation. In *Comprehensive Mechanics of Materials*, pp. 3–56. Elsevier, Oxford, 1st edition, 2024.